Spectral line profile of self-broadened CO_2 from the center to the far wing

O.B. Rodimova

Institute of Atmospheric Optics,
Siberian Branch of the Russian Academy of Sciences, Tomsk

Received July 29, 2002

An equation for the spectral line profile derived within the framework of the far-wing line shape theory is used to retrieve a single set of parameters using the nonlinear least-square method. The corresponding line shape describes experimental data pertaining to the pure CO_2 gas at different temperatures in various spectral ranges. The HITRAN-86 database of spectral line characteristics serves a source of initial spectroscopic information. The obtained sets of parameters referred to the quantum and classical intermolecular interaction potentials describe experimental data on the spectral and temperature dependence of the absorption coefficients in wings of the CO_2 1.4, 2.7, 4.3, and 15-μm bands with the experimental accuracy.

1. Theoretical approaches to description of absorption in far wings

The shape of spectral line in its central part is now studied rather thoroughly. At ordinary temperatures and pressures, it is described by the Lorentz profile:

$$\kappa(\omega) \sim \frac{S}{\pi} \frac{\alpha}{\alpha^2 + (\omega - \omega_0)^2}, \qquad (1)$$

where S is the line strength; α is the line halfwidth; ω_0 is the central frequency of the line, and ω is the current frequency. It is also known that the line shape in a wing differs from the Lorentz one. In the near wing it can exceed the Lorentz profile, passing on to the exponential decrease in the far wing. In spite of much attention paid by investigators to the problem of line shape in the far wings, by now there is no some unified idea concerning this problem in the literature and different authors continue to use different theoretical models.

A physical system to be considered in the problem of light absorption is a macroscopic body of a matter consisting of N molecules. It includes the molecule–radiation and intermolecular interactions, so quantum equations for it, although being rather simple in form, cannot be solved directly. Traditionally, the following simplifications are made. First of all, the active molecule absorbing the radiation is distinguished from other buffer molecules determining the statistical situation, that is, the resulting correlation function of the dipole moment $\Phi(t)$ includes the statistical part and the part corresponding to interaction between two molecules. One of the possible approaches is a construction of model correlation functions (see, for example, Refs. 1 and 2). Within calculation of the correlation function, there exist two theoretically equivalent approaches to calculation of the absorption coefficient – the use of kinetic equations for the correlation function of the dipole moment and the method of resolvent.[3–5]

The next natural simplification is a transition to small or large frequency detunings. In the first case, the assumption that the collision is instantaneous just leads to the Lorentz (dispersion) line shape. For large frequency detunings, certain assumptions on interaction with buffer molecules are needed. In the statistical approximation, the molecular environment is considered as a source of stationary perturbation of energy levels of the active (absorbing) molecule, while other molecules are assumed fixed at some separation R from the active one. In this case, the line shape equation at asymptotic transition to large frequency shifts includes an exponential factor

$$\kappa(\omega) \sim |\omega - \omega_0|^{-a}, \qquad (2)$$

characterizing the so-called statistical profile. The idea of statistical description (quasistatic approximation) within the resolvent method at classical coordinates of nuclei was successfully used by Rosenkranz[6,7] to describe absorption in line wings as applied to the 8–12-μm water vapor window. It received further development in the papers by Ma and Tipping (see, for example, Refs. 8, 9, and references therein). However, the transition from the fully quantum problem to the semiclassical version in the quasistatic approximation in these papers is actually made through declaration of intermolecular separation as a parameter in the complete Hamiltonian, that is not satisfactory from the viewpoint of consistent theoretical description.

0235-6880/02/09 694-10 $02.00

More rigorous version of transition to the semiclassical description, when the motion of molecular centers of gravity is considered classically, while the binary problem remains quantum, is realized in the line wing theory[10–13] using the method of semiclassical representation[14] in the formalism of kinetic equations. The kinetic equation was derived for the correlation function of the dipole moment such that asymptotic cases for the large and small frequency detunings were separated in the equation itself.[13,15] A single analytical equation for the absorption line profile cannot be obtained *ab initio* for all frequency detunings $\Delta\omega$. Therefore, two asymptotic cases: line center (small $\Delta\omega$) and line wing (large $\Delta\omega$) are considered separately.

In the theory of line wings, the general kinetic equation is written for large $\Delta\omega$ and the quantum problem appearing in it for the interacting active and buffer molecules is considered at classical motion of the centers of gravity. The spectral absorption coefficient is expressed through the kinetic equation solution accurate to a factor as

$$\kappa(\omega) = \mathrm{Re}\,\mathrm{Tr}_x MQ = \sum_{n,n'} M_{n'n}\,\mathrm{Re}\,Q_{nn'}\,, \qquad (3)$$

where M is the dipole moment of the active (interacting with the field) molecule; Tr_x is the spur operation with respect to intramolecular variables x; the matrix elements $(\ldots)_{nn'} \equiv \langle n|\ldots|n'\rangle$ include eigenfunctions $|n\rangle$ of the Hamiltonian $H_1(x)$ of the active molecule. The kinetic equation for $Q_{nn'}$ in the asymptotic case of large frequency detunings has the form

$$i(\omega - \omega_{nn'})\,Q_{nn'} + M_{nn'}\,\rho^{(1)}_{n'} = (\omega - \omega_{nn'})^2\,(\hat{Y}\,Q)_{nn'} \quad (4)$$

with the superoperator $\hat{Y}$ describing the interaction of the active molecule with the environment. In Eq. (4) $\omega_{nn'} = (W^{(1)}_n - W^{(1)}_{n'})/\hbar$, $W^{(1)}_n$ are eigenvalues of H_1; $\rho^{(1)}_n \equiv \langle n|\rho^{(1)}|n\rangle$ for the Gibbs density matrix $\rho^{(1)}$ of the active molecule:

$$\mathrm{Re}\,Q_{nn'} = (\omega - \omega_{nn'})\sum_{n_1,n_2}(\mathrm{Re}\,Y_{nn',n_1n_2})\frac{M_{n_1n_2}\rho^{(1)}_{n_2}}{\omega - \omega_{nn'}}\,, \qquad (5)$$

$$\mathrm{Re}\,Y_{nn',n_1n_2} = \mathrm{Re}\int_0^\infty \mathrm{d}t e^{i\omega t}\times$$

$$\times\sum_{\alpha\alpha'}(\langle n\alpha|\hat{S}|n_1\alpha'\rangle\,\rho^{(2)}_\alpha\,\langle n_2\alpha'|\hat{S}^{-1}|n'\alpha\rangle)_{st}; \qquad (6)$$

$$i\hbar\frac{\partial\hat{S}}{\partial t} = \{H_1(x) + H_2(y) + U[x, y(\mathbf{r}(t))]\}\,\hat{S}. \qquad (7)$$

Equation (7) is the temporal binary Schrödinger equation for quantum states of the active and buffer molecules (y are intramolecular degrees of freedom of the latter) at the classical motion of the centers of gravity ($\mathbf{r}(t)$ is the vector connecting the centers of gravity); $H_2(y)$ is the Hamiltonian of the buffer molecule; $\rho^{(2)}$ is its Gibbs density matrix; $\hat{S}$ is the evolution operator; $|\alpha\rangle$ are eigenfunctions of H_2; $U(x, y|\mathbf{r}(t))$ is the Coulomb energy of intermolecular interaction. Then the temporal binary problem (7) is solved through eigenfunctions and eigenvalues of the stationary problem, which includes time as a parameter

$$(H_1 + H_2 + U)\,\chi_{n\alpha}(t) = W_{n\alpha}(t)\,\chi_{n\alpha}(t). \qquad (8)$$

The solution includes the energy difference between the interacting molecules. When the solution is substituted into the equation for the absorption coefficient, the integral arises, which is estimated asymptotically at large frequency detunings, giving the δ-function because of this difference:

$$\int_0^{t^*}\mathrm{d}t\,\exp\left[i\omega t + \frac{1}{i\hbar}\int_0^t[W_{n''\alpha''}(t') - W_{n'\alpha'}(t')]\mathrm{d}t'\xi(t)\right]\rightarrow$$

$$\rightarrow \delta(\omega - \omega_{n_1n_2} - \omega_{n_1n_2\alpha'}), \qquad (9)$$

$$\omega_{n_1n_2\alpha'} = (1/i\hbar)(\tilde{W}_{n_1\alpha} - \tilde{W}_{n_2\alpha}).$$

As a result, the classical problem should be considered only in the vicinity of just this point. The operation of statistical averaging gives an exponent with the potential of the classical problem. The calculation is exact until this point. Then the following approximations are introduced.

In the vicinity of the point, where absorption occurs, the actual trajectory is approximated by a straight-line part

$$r(t) = \sqrt{r^2 + v^2|t - t_0|^2}\,. \qquad (10)$$

The quantum problem for $W_{n\alpha}$ is not solved, but parameterized, and the constants $C_{j\nu j'\nu'\alpha}$ and a arise:

$$\omega_{j\nu j'\nu'\alpha} = \frac{C_{j\nu j'\nu'\alpha}}{r^a}\,. \qquad (11)$$

The constant D denotes combinations of matrix elements of the quantum problem of intermolecular interactions:

$$D = 32\,\frac{\pi^2}{a}\,\frac{\sqrt{m_1m_2}}{m_1 + m_2}\times$$

$$\times\sum_{\nu\nu'}\sum_\alpha\rho^{(2)}_\alpha\,\frac{|M_{j\nu j'\nu'}|^2}{\sum\limits_{\nu\nu'}|M_{j\nu j'\nu'}|^2}\,|C_{j\nu j'\nu'\alpha}|^{3/a} +$$

$$+\sum_{\nu_1}|C_{j\nu_1 j'\nu'\alpha}|^{3/a}\left|\frac{M_{j\nu_1 j'\nu'}}{M_{j\nu j'\nu'}}\right|^2\frac{\langle j\nu\alpha|U\tilde{\Omega}_+|j\nu_1\alpha\rangle}{V} +$$

$$+\sum_{\nu_2}\left|C_{j\nu j'\nu_2\alpha}\right|^{3/a}\left|\frac{M_{j\nu j'\nu_2}}{M_{j\nu j'\nu'}}\right|^2\frac{\langle j'\nu_2\alpha|\tilde{\Omega}_+^*U|j'\nu'\alpha\rangle}{V}+$$

$$+\sum_{\nu_1\nu_2}\left|C_{j\nu_1 j'\nu_2\alpha}\right|^{3/a}\left|\frac{M_{j\nu_1 j'\nu_2}}{M_{j\nu j'\nu'}}\right|^2\times$$

$$\times\frac{\langle j\nu\alpha|U\tilde{\Omega}_+|j\nu_1\alpha\rangle\langle j'\nu_2\alpha|\tilde{\Omega}_+^*U|j'\nu'\alpha\rangle}{V^2}. \qquad (12)$$

In Eq. (12) $n \to j\nu$, j numbers energy levels, ν is the degeneration index; $\tilde{\Omega}_+, \tilde{\Omega}_+^*$ are the Möller operators connecting the initial and the final states in the process of molecular interaction; V is the classical potential of intermolecular interaction; $\frac{m\mathbf{v}_0^2}{2}-\frac{m\mathbf{v}'^2}{2}=V(\mathbf{r}_{\min})$, $\mathbf{v}_0$, $\mathbf{v}'$ are the initial velocity of the center of gravity and the velocity at the point $\mathbf{r}_{\min}$ – the point of maximum approach of the molecules at the classical trajectory; m_1 and m_2 are masses of the active and buffer molecules.

Thus, the final equation for the absorption coefficient includes the known physical parameters: the quantum potential of intermolecular interaction, which is approximated as ~ C_a/R^a at different parts of the potential curve, and the so-called classical potential of intermolecular interaction $V(R)$, which follows from the former through a certain averaging procedure.

2. Equation for line shape in the far-wing theory

The absorption coefficient at frequency ω conditioned by the absorption in an individual jth line, centered at ω_j with the separation between the molecules corresponding to the C_a/R^a approximation of the quantum potential of intermolecular interaction, has the form

$$\kappa_a(\omega) \sim S_j G_W(\omega, \omega_j, T, P) =$$

$$= S_j D_{aj}\frac{1}{|\omega-\omega_j|^{1+3/a}}\frac{1}{r_j}\int_0^{r_j}\frac{e^{-V(r,T)/kT}}{\sqrt{r_j^2-r^2}}r\,dr =$$

$$= S_j D_{aj}\frac{1}{|\omega-\omega_j|^{1+3/a}}F(r_j), \qquad (13)$$

where

$$r_j=\frac{C_a}{|\omega-\omega_j|^{1/a}};\quad D_{aj}=D_a\gamma_j; \qquad (14)$$

$$F(r_j)=\frac{1}{r_j}\int_0^{r_j}\frac{e^{-\frac{V(r,T)}{kT}}r\,dr}{\sqrt{r_j^2-r^2}}; \qquad (15)$$

j numbers individual lines; S_j is the line strength. The equation for line shape calculation is a piecewise continuous function according to the approximation of the quantum potential, every part of which corresponds to a certain value of a:

$$\kappa(\omega)=$$

$$=\begin{cases}\kappa_{\mathrm{Lor}}(\omega), & \Delta\omega<\Delta\omega_{\min 1}\\ \left.\begin{matrix}\kappa_{\mathrm{Lor}}(\omega), & \kappa_{\mathrm{Lor}}(\omega)>\kappa_{a_1}(\omega)\\ \kappa_{a_1}(\omega), & \kappa_{\mathrm{Lor}}(\omega)<\kappa_{a_1}(\omega)\end{matrix}\right\} & \Delta\omega_{\min 1}<\Delta\omega<\Delta\omega_{\min 2}\\ \left.\begin{matrix}\kappa_{a_1}(\omega), & \kappa_{a_1}(\omega)>\kappa_{a_2}(\omega)\\ \kappa_{a_2}(\omega), & \kappa_{a_1}(\omega)<\kappa_{a_2}(\omega)\end{matrix}\right\} & \Delta\omega_{\min 2}<\Delta\omega<\Delta\omega_{\min 3}\\ \left.\begin{matrix}\kappa_{a_2}(\omega), & \kappa_{a_2}(\omega)>\kappa_{a_3}(\omega)\\ \kappa_{a_3}(\omega), & \kappa_{a_2}(\omega)<\kappa_{a_3}(\omega)\end{matrix}\right\} & \Delta\omega>\Delta\omega_{\min 3}\end{cases} \qquad (16)$$

The parameters of such a combined shape can be determined from comparison of experimental and calculated data. As a rule, certain terms of C_a/R^a are associated with experimental data in certain frequency intervals, so the corresponding parameters can be found, in some cases, independently for different spectral intervals. A typical profile of a spectral line with allowance for its behavior in the line wing is shown in Fig. 1.

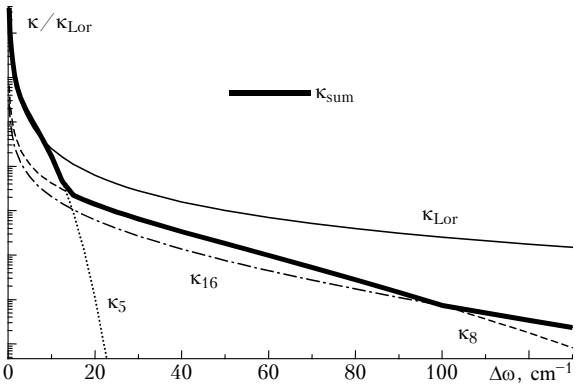

Fig. 1. Combined profile for the CO_2 4.3-μm band at self-broadening.

As can be seen, different parts of the wing alternate each other as one of them begins to exceed another.

The classical potential of intermolecular interaction $V(R, T)$ depends on temperature, and calculations usually deal with the Lennard–Jones potential. It enters into the function $F(R)$, which serves a factor in the absorption coefficient and determines, to a large degree, the spectral and temperature dependence of the absorption coefficient.

The theory of line wings has been developed by us and used for interpretation of spectral data on absorption in line and band wings for more than 25 years. It should be emphasized that the line shape parameters in the equation are connected only with the intermolecular interaction potential and can be found through minimization of the discrepancy between the calculated and experimental values of the absorption coefficient. Using this theory, we have interpreted the experimental data (as they appeared) on wing absorption by various gases in different spectral ranges and at different temperatures. A particular attention was paid

to CO_2 absorption, especially, in the 4.3-μm band, because the wing of this band is thoroughly studied experimentally. Earlier the line shape (i.e., potential) parameters were determined by manual fitting with allowance for the limited number of lines in the band. The current situation in the spectroscopy implies the use of spectroscopic databases. Therefore, recently we attempted to use the available absorption data to determine by the least-square method a single set of parameters describing the whole variety of experimental data for a certain gas mixture in the absorption band under consideration. The HITRAN database was used as a source of initial information.[18]

The absorption coefficient at frequency ω conditioned by absorption in all lines lying within $\pm \Delta\omega_{\text{lim}}$ from the center of each line can be written as

$$\kappa(\omega, T, P) = \sum_j \frac{\omega}{\omega_j} \frac{(1 - e^{-\hbar\omega / kT})}{(1 - e^{-\hbar\omega_j / kT})} \times \times S_j(T)\, G(\omega, \omega_j, T, P). \quad (17)$$

Databases contain spectral line characteristics for a certain temperature T_0. In the HITRAN database[18] $T_0 = 296$ K. Then the strength of the jth line at an arbitrary temperature T is

$$S_j(T) = S_j(T_0) \frac{(1 - e^{-\hbar\omega_j / kT})}{(1 - e^{-\hbar\omega_j / kT_0})} \times \times \exp\left[- C_2 E_j \frac{(T_0 - T)}{T_0 T} \right] \frac{Q_v(T_0)}{Q_v(T)} \frac{Q_R(T_0)}{Q_R(T)}, \quad (18)$$

where Q_v and Q_R are the vibrational and rotational statistical sums, respectively; E_j (cm^{-1}) is the energy of the lower energy level in a transition; $[S] = \text{cm}^{-1}/(\text{cm}^{-2} \cdot \text{mol})$; $C_2 = hc/k = 1.439$ cm·deg. For CO_2 $Q_R(T_0)/Q_R(T) \sim (T_0/T)$ and the absorption coefficient κ ($\text{cm}^2 \cdot \text{mol}^{-1}$) has the form

$$\kappa(\omega, T, P) = \sum_j \frac{\omega}{\omega_j} \frac{(1 - e^{-\hbar\omega / kT})}{(1 - e^{-\hbar\omega_j / kT_0})} S_j(T_0) \times \times \exp\left[- C_2 E_j \frac{(T_0 - T)}{T_0 T} \right] \frac{Q_v(T_0)}{Q_v(T)} \left(\frac{T_0}{T} \right) G(\omega, \omega_j, T, P). \quad (19)$$

At rather small ω_j, when the line central frequency becomes comparable with the frequency detuning, the line shape equation should include the term with the sum frequency, that is,

$$G(\omega, \omega_j, T, P) = G^-(\omega, \omega_j, T, P) + + e^{-\hbar\omega_j / kT} G^+(\omega, \omega_j, T, R). \quad (20)$$

This should be taken into account, for example, for the CO_2 15-μm band. Otherwise, it is assumed in Eq. (19) that

$$G(\omega, \omega_j, T, P) = G^-(\omega, \omega_j, T, P).$$

Below we present the CO_2 absorption coefficients calculated in the case of self-broadening with the use of Eqs. (13)–(20) in minimization of parameters a, C_a, and D_a for the 1.4, 2.7, 4.3, and 15-μm bands.

3. CO_2 absorption at self-broadening in wings of the 4.3-μm band at different temperatures

The spectral interval in the wing of the CO_2 4.3-μm band plays a special role in studies of wings of the molecular IR spectra. The exponential behavior of κ(ω) in the far wing was found for the first time just in that interval. The spectral behavior of κ(ω) and the dependence of κ(ω) on the type of the buffer gas are well studied, and the temperature dependence κ(ω, T) is now a subject of investigations (see, for example, Refs. 19–22). To be noted are also some of numerous calculations of absorption in this spectral range.[9,22] A detailed review of experimental and theoretical papers dealing with the CO_2 4.3-μm band wing can be found in Ref. 23.

The wing theory was first applied to the study of absorption by water vapor in the region 8–12 μm and by carbon dioxide in the 4.3-μm band wing in Ref. 10, which, in essence, laid the groundwork for understanding physics of the process under study and did not lose its importance by now. Then, in some papers (see Refs. 13, 16, 17, 23 and references therein), the theory, terminology, and parameters were refined. The important part in the development of the theory play the concepts of the key role of the repulsive branch of the quantum intermolecular interaction potential in the absorption and the possibility of its approximation by a set of terms with the inverse dependence on the separation, as well as the idea on the temperature dependence of the classical potential. Earlier, the parameters were found by us by manual fitting for the CO_2 4.3-μm band in different spectral intervals at different temperatures. Within the above scheme, we always succeeded in fitting such shape parameters that agreed with the experimental data within the experimental uncertainty. However, it was difficult to fit simultaneously the wing and microwindow parameters at different temperatures. In this paper, an attempt is made to use the available data on absorption for to find, using the least square method, a single set of parameters describing the whole variety of available measurements for a certain gas mixture.

To be noted first of all is the role of the function $F(R)$ in description of absorption in the wing of the CO_2 4.3-μm band. Figure 2 depicts the ratio of the experimental coefficients for different mixtures[22,26] and the ratios of the corresponding functions $F(R)$. Their qualitative similarity allows us to state that just these functions reflect the most significant features inherent in absorption for different gas mixtures. Also note that,

besides the temperature dependence of the line strength, the temperature dependence of the absorption coefficient is mostly determined by the classical intermolecular interaction potential $V(R)$ taken in calculations in the form of the Lennard–Jones potential entering into the function $F(R)$, whose parameters are just temperature-dependent (Fig. 3).

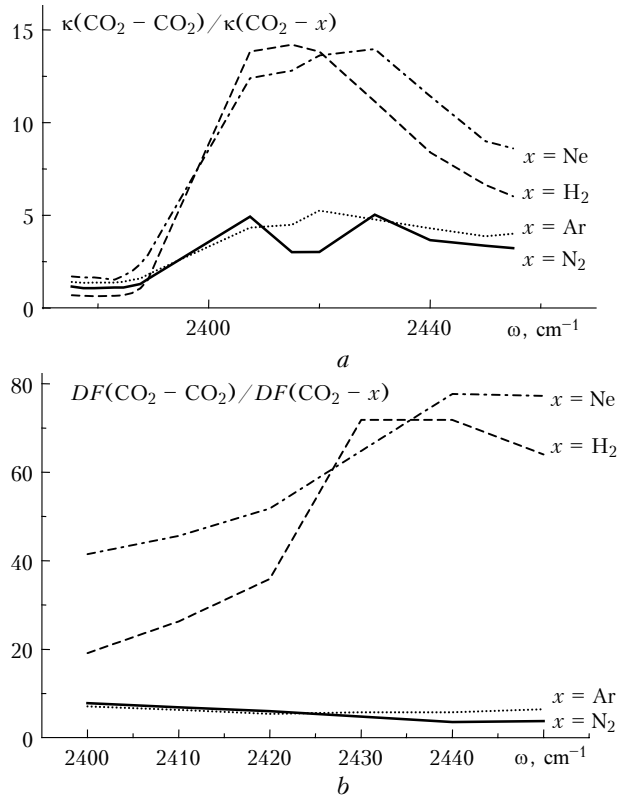

Fig. 2. Ratios of experimental CO_2 absorption coefficients in the wing of the 4.3-μm band for different buffer gases. Self-broadening experimental data are borrowed from Ref. 26, other data are taken from Refs. 22 and 26 (*a*); the ratios of the function F in the wing of the CO_2 4.3-μm band for different buffer gases as estimated at $a = 10$ (*b*).

Parameters of the quantum potential are determined stage-by-stage. Description of the data in the wing of the 2400–2500-cm^{-1} band at the normal temperature requires mostly the far-wing parameters ($a = 8$ and 16) to be known, and just these parameters are determined from minimization at some given C_5 and D_5, as well as ε and σ in the Lennard–Jones potential taken from thermodynamic measurements. The next stage is the determination of C_5 and D_5 from the absorption data in microwindows within the 2350–2400-cm^{-1} band at predetermined C_8, D_8, C_{16}, and D_{16}. The constants $\Delta\omega_{min2}$ and $\Delta\omega_{min3}$ are introduced to avoid unnecessary comparisons, the constant $\Delta\omega_{min1}$ determines the transition from the Lorentz center to a near wing and may depend on pressure. The absorption data in the far wing at different temperatures serve for determining the classical potential parameters ε and σ, which thus turn out to be temperature-dependent.

The first row of Table 1 gives the values of the shape parameters for lines in the CO_2 4.3-μm band. These parameters were obtained from manual fitting[24] (see also Refs. 13 and 25) and then through the above procedure using the nonlinear least-square method for the bands considered.

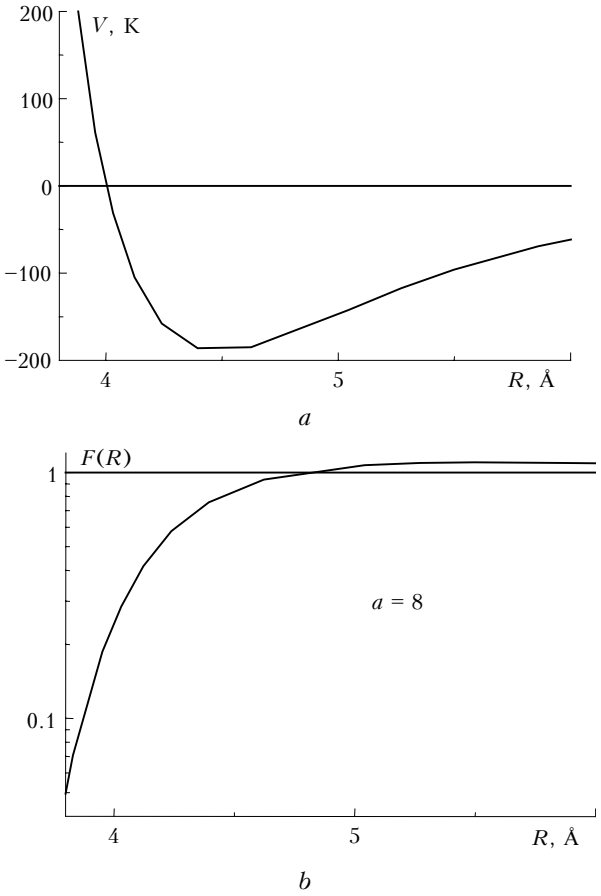

Fig. 3. Classical intermolecular interaction potential taken for CO_2 in the form of the Lennard–Jones potential, $4\varepsilon/k = 760$ K, $\sigma = 4.0$ Å (*a*); function $F(R)$ determining the line shape in a wing (*b*).

Table 1. Parameters of quantum potential for different CO_2 bands

Band, μm	C_5	D_5	C_8	D_8	C_{16}	D_{16}	C_{20}	D_{20}
4.3	6.5	0.2	6.73	0.015	5.0601	0.0053	–	–
4.3	6.5906	0.18468	6.722	0.011222	5.0368	0.005509	–	–
1.4	–	–	6.722	0.022	5.0369	0.005486	–	–
2.7	–	–	6.722	0.014	5.0369	0.009	4.88	0.005
15	6.5	0.0005	7.6	0.00000665	–	–	–	–

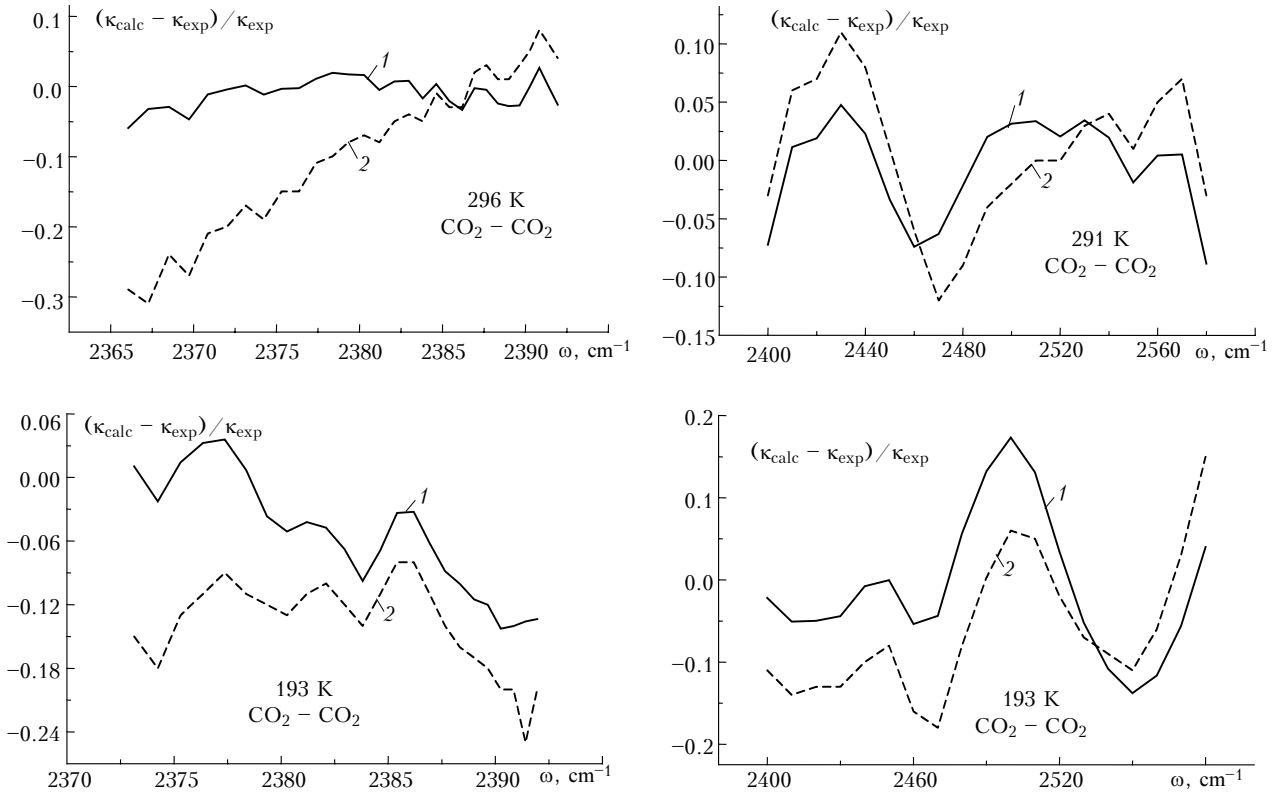

Fig. 4. Deviations of calculated absorption coefficients from experimental ones in the CO_2 4.3-μm band: in microwindows (to the left) and in the wing (to the right); calculation by the least-square method (curves *1*) and manual fitting (curves *2*).

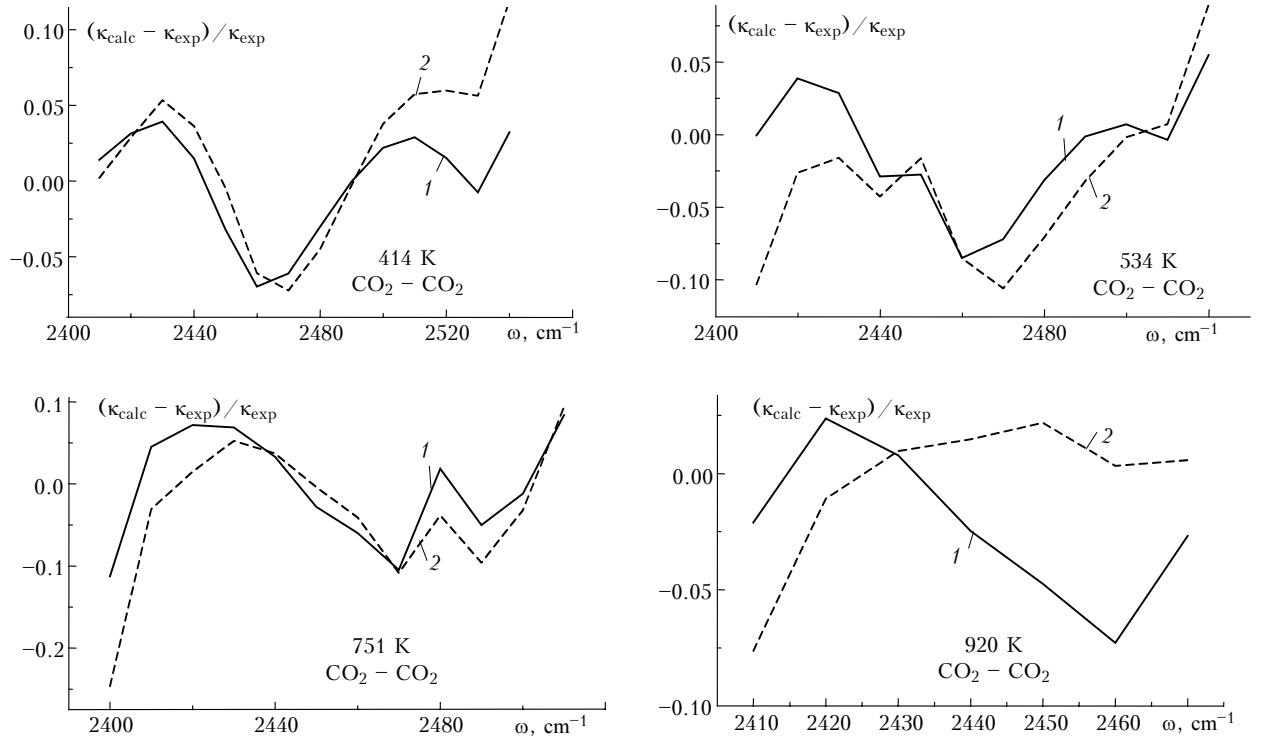

Fig. 5. Deviations of calculated absorption coefficients from experimental ones in the wing of the CO_2 4.3-μm band at high temperature; calculation by the least-square method (curves *1*) and manual fitting (curves *2*).

Figure 4 shows the deviations of the calculated absorption coefficients from experimental ones for microwindows[27] and the wing of the CO_2 4.3-μm band[26] at the normal and low temperatures. Figure 5 depicts the deviations of the calculated absorption coefficients from experimental ones[28,29] for the wing of the CO_2 4.3-μm band at a high temperature. The quantum interaction potential, approximated as $\Delta E_a \sim \Delta\omega_a = (C_a/R)^a$, with the parameters used in calculations is shown in Fig. 6.

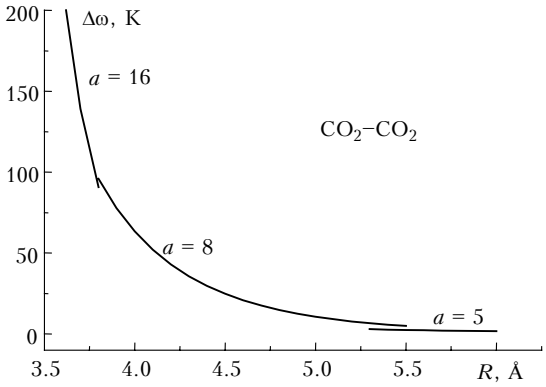

Fig. 6. Quantum interaction potential approximated as $\Delta E \sim \Delta\omega = (C/R)^a$ in calculations.

On the scale of the figure, it almost coincides with that obtained earlier by manual fitting. The temperature behavior of the classical potential parameters ε and σ is depicted in Fig. 7.

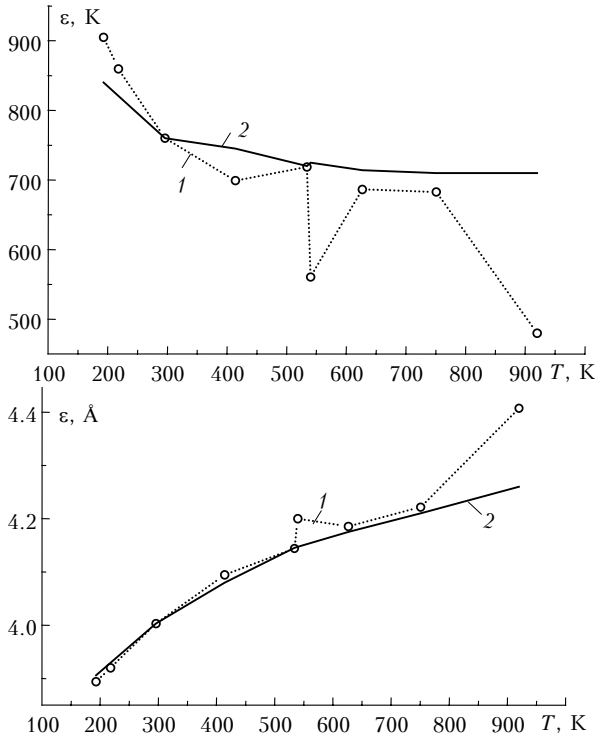

Fig. 7. Parameters ε and σ of the classical intermolecular interaction potential as functions of temperature: calculation by the least-square method (curves *1*) and manual fitting (curves *2*).

The relatively smooth curves in the case of manual fitting show spikes at some temperature values at minimization by the nonlinear least-square method. This is due to the fact that the surface of the sum of the square errors in the coordinates of ε and σ, which is minimized to determine the sought parameters, is almost constant in a wide range of parameters (Fig. 8).

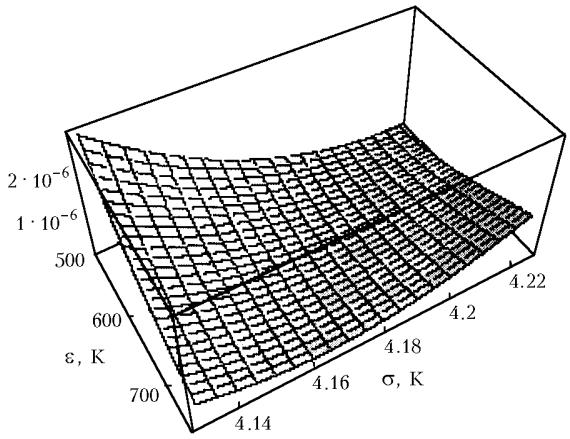

Fig. 8. Surface of the sum of square errors in coordinates of ε and σ for T = 540 K.

In other words, we determine in fact only some range of parameters, in which we can again choose a smooth curve. In this case, for arbitrary temperatures from the studied interval of their values, the corresponding potential parameters can be selected, as it was done for the temperature T = 920 K (see Ref. 30), when the corresponding experimental data[29] were still unknown.

4. CO_2 absorption at self-broadening in wings of the 1.4 and 2.7-μm bands

The absorption coefficients in comparison with experimental ones[20] at the ordinary temperature are shown in Figs. 9 and 10 for the wings of the CO_2 1.4 and 2.7-μm bands. The corresponding parameters of the quantum potential are given in Table 1. Note that in the case of the 2.7-μm band we have to extend the approximation of the potential to larger separations (C_{20}, D_{20}). It can be seen that the parameters corresponding to line wings (C_8, C_{16}) are the same for the 4.3, 2.7, and 1.4-μm bands. These three bands have the same initial state – the ground state (0, 0^0, 0) – and different final states (Table 2).

The shape constant C_a in the equation $\omega_{n_1n_2\alpha} = C_{n_1n_2\alpha}/r^a$ corresponds to the energy difference between the interacting molecules [see Eq. (9), where the energy of interaction of the active molecule in the state n_1 with the buffer molecule in the state α is $\tilde{W}_{n_1\alpha}$].

Table 2. Characteristics of CO_2 absorption bands

Band, μm	Spectral range, cm^{-1}	Transition
15	800	$(1, 0^0, 0) \xrightarrow{\nu_2} (0, 1^1, 0)$
4.3	2400	$(0, 0^0, 0) \xrightarrow{\nu_3} (0, 0^0, 1)$
2.7	3800	$(0, 0^0, 0) \xrightarrow{\nu_1+\nu_3} (1, 0^0, 1)$
1.4	7000	$(0, 0^0, 0) \xrightarrow{3\nu_3} (0, 0^0, 3)$

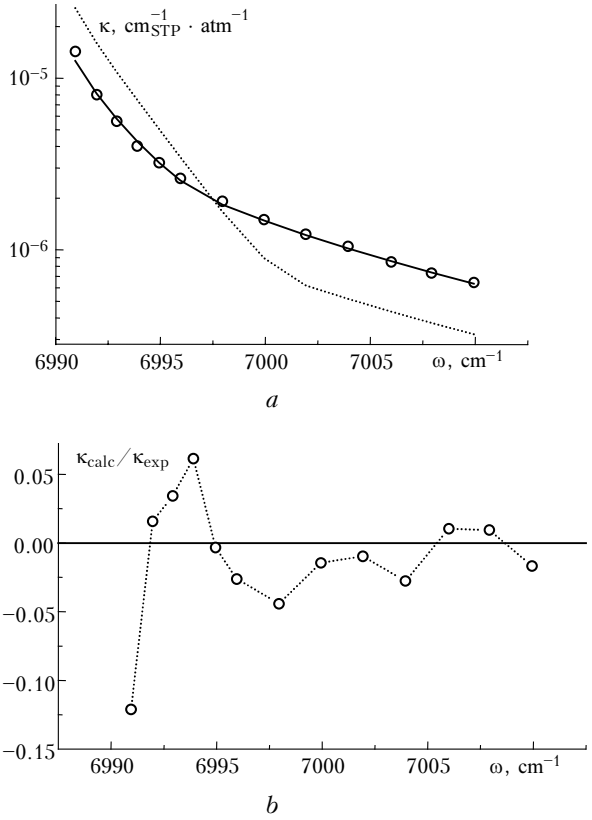

Fig. 9. Absorption in the wing of the CO_2 1.4-μm band at $T = 296$ K: absorption coefficient (*a*): experimental data[20] (circles), absorption coefficient calculated with the shape for the 4.3-μm band (dashed curve), calculation with the shape for the 1.4-μm band (solid line); deviations of the calculated absorption coefficients from experimental ones (*b*).

The equality of constants C_a for different bands means that the corresponding energy differences are such that a radiation quantum is absorbed at roughly the same separation between the interacting molecules. The constant D_a is a complex combination of matrix elements (12), which in the absence of interference can be reduced to the following equation

$$D_a \propto \left(32\pi^2/a\right)\sqrt{m_1 m_2}\,(m_1 + m_2)^{-1} C^{3/a} \left| \frac{\langle M \rangle}{\sum \langle M \rangle} \right|^2$$

for a structureless buffer molecule. The relation between matrix elements of the dipole moment just can result in different D_a constants. The behavior of D_a from one band to another (see Table 1) has a tendency to growth as the transition energy increases.

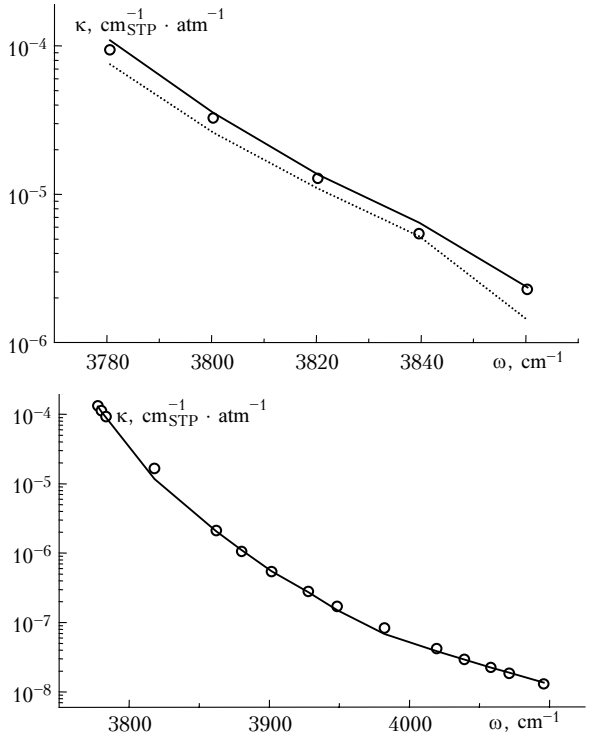

Fig. 10. Absorption in a wing of the CO_2 2.7-μm band at $T = 296$ K for different spectral intervals: experimental data[20] (circles), absorption coefficient calculated with the shape for the 4.3-μm band (dashed curve), calculation with the shape for the 2.7 μm band (solid line).

5. CO_2 absorption at self-broadening under different temperatures in wing of the 15-μm band

The calculated and experimental[31] absorption coefficients in the wing of the CO_2 15-μm band are compared in Fig. 11.

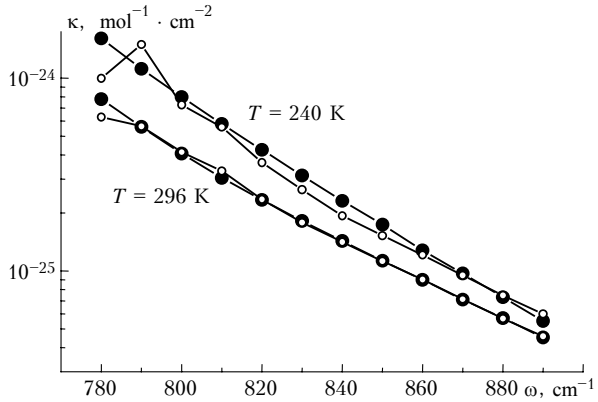

Fig. 11. Absorption coefficient in the wing of the CO_2 15-μm band: calculation (open circles) and experimental data[31] (closed circles).

Parameters of the corresponding quantum potential are given in Table 1. The 15-μm band corresponds to the vibrational state different from those considered above. Therefore, the constants D_i are expected to be small because of the low transition energy, and this comes true in practice.

Conclusion

The available sets of parameters provide description of experimental data on the absorption coefficient in wings of the CO_2 1.4, 2.7, 4.3, and 15-μm bands depending on the frequency, temperature, and the type of the buffer gas accurate to the experimental uncertainty with the use of the HITRAN database.[18]

The Benedict profile[19] obtained from analysis of experimental data on the absorption coefficient in the 4.3-μm band is still often used in calculations of radiation characteristics when studying absorption in line wings. It should be emphasized here that the shape of a spectral line changes significantly from one band to another. As an example, Fig. 12 depicts the shapes of lines belonging to the 4.3 and 15-μm bands.

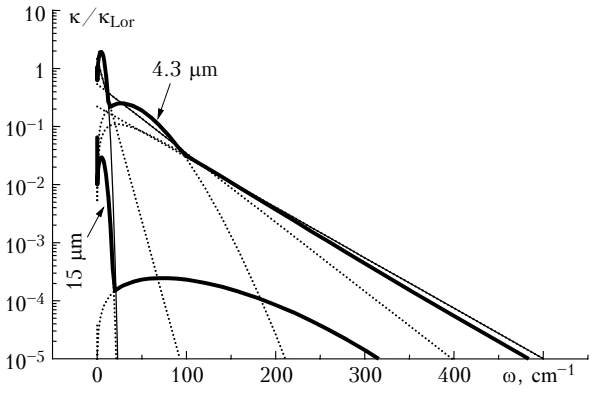

Fig. 12. Comparison of line shapes for the CO_2 4.3 and 15-μm absorption bands and the empiric profile[26] for the 4.3-μm band: profile calculated by the line wing theory for the 4.3 and 15-μm bands (thick lines); empiric profile for the 4.3-μm band (thin line).

It should be also kept in mind that the use of some other databank in place of HITRAN[18] can somewhat change the potential parameters. However, this change can hardly be significant, as can be judged from Table 1 that presents the data on the change of the parameters at transition from the use of 100 basic lines of the 4.3 μm band to the use of the HITRAN database.[18]

The analytical equation for the line shape in the asymptotic case of large frequency detunings is a little bit more complicated than the Lorentz profile for small frequency detunings. This allows it to be used in the studies of radiation conditions on different planets. The wing range of the 15-μm band is very important for conditions of the Earth's and Mars's atmospheres, and the range of the 4.3-μm band is of significance for calculations of the Venus's radiation conditions.

Acknowledgments

The author is grateful to S.D. Tvorogov and L.I. Nesmelova for continuous and fruitful cooperation and constructive criticism.

This work was partly supported by the Russian Foundation for Basic Research (Grant No. 00–05–65209).

References

1. G. Birnbaum, J. Quant. Spectrosc. Radiat. Transfer **21**, No. 6, 597–607 (1979).
2. R. Armstrong, J. Quant. Spectrosc. Radiat. Transfer **28**, No. 4, 297–304 (1982).
3. U. Fano, Phys. Rev. **131**, No. 1, 259–268 (1963).
4. R. Zwanzig, J. Chem. Phys. **33**, No. 5, 1338–1341 (1960).
5. I.I. Sobelman, *Introduction to Theory of Atomic Spectra* (Fizmatgiz, Moscow, 1963), 640 pp.
6. P.W. Rosenkranz, J. Chem. Phys. **83**, No. 12, 6139–6144 (1985).
7. P.W. Rosenkranz, J. Chem. Phys. **87**, No. 1, 163–170 (1987).
8. Q. Ma and R.H. Tipping, J. Chem. Phys. **111**, No. 13, 5909–5921 (1999).
9. Q. Ma, R.H. Tipping, C. Boulet, and J.-P. Bouanich, Appl. Opt. **38**, No. 3, 599–604 (1999).
10. S.D. Tvorogov and L.I. Nesmelova, Izv. Akad. Nauk SSSR, Ser. Fiz. Atmos. Okeana **12**, No. 6, 627–633 (1976).
11. L.I. Nesmelova, S.D. Tvorogov, and V.V. Fomin, *Spectroscopy of Line Wings* (Nauka, Novosibirsk, 1977), 141 pp.
12. V.V. Fomin, *Molecular Absorption in Infrared Atmospheric Windows* (Nauka, Novosibirsk, 1986), 234 pp.
13. L.I. Nesmelova, O.B. Rodimova, and S.D. Tvorogov, *Spectral Line Shape and Intermolecular Interaction* (Nauka, Novosibirsk, 1986), 216 pp.
14. E.P. Gordov and S.D. Tvorogov, *Method of Semiclassical Representation of Quantum Theory* (Nauka, Novosibirsk, 1984), 167 pp.
15. S.D. Tvorogov and O.B. Rodimova, J. Chem. Phys. **102**, No. 22, 8736–8745 (1995).
16. L.I. Nesmelova, O.B. Rodimova, and S.D. Tvorogov, Izv. Vyssh. Uchebn. Zaved., Ser. Fizika, No. 10, 106–107 (1980).
17. L.I. Nesmelova, O.B. Rodimova, and S.D. Tvorogov, in: *Spectroscopy of Atmospheric Gases* (Nauka, Novosibirsk, 1982), pp. 4–16.
18. L.S. Rothman, R.R. Gamache, A. Goldman, L.R. Brown, R.A. Toth, H.M. Pickett, R.L. Poynter, J.-M. Flaud, C. Camy-Peyret, A. Barbe, N. Husson, C.P. Rinsland, and M.A.H. Smith, Appl. Opt. **26**, No. 19, 4058–4097 (1987).
19. B.H. Winters, S. Silverman, and W.S. Benedict, J. Quant. Spectrosc. Radiat. Transfer **4**, No. 4, 527–537 (1964).
20. D.E. Burch, D.A. Gryvnak, R.R. Patty, and Ch.E. Bartky, J. Opt. Soc. Am. **59**, No. 3, 267–280 (1969).
21. J. Boissoles, C. Boulet, J.M. Hartmann, M.Y. Perrin, and D. Robert, J. Chem. Phys. **93**, No. 4, 2217–2221 (1990).

22. M.O. Bulanin, A.B. Dokuchaev, M.V. Tonkov, and N.N. Filippov, J. Quant. Spectrosc. Radiat. Transfer **31**, No. 6, 521–543 (1984).
23. L.I. Nesmelova, O.B. Rodimova, and S.D. Tvorogov, Opt. Atm. **1**, No. 5, 3–18 (1988).
24. L.I. Nesmelova, O.B. Rodimova, and S.D. Tvorogov, Atmos. Oceanic Opt. **5**, No. 9, 609–614 (1992).
25. L.I. Nesmelova, O.B. Rodimova, and S.D. Tvorogov, Izv. Vyssh. Uchebn. Zaved., Ser. Fizika, No. 5, 54–58 (1982).
26. R. Le Doucen, C. Cousin, C. Boulet, and A. Henry, Appl. Opt. **24**, No. 6, 897–906 (1985).
27. C. Cousin, R. Le Doucen, C. Boulet, A. Henry, and D. Robert, J. Quant. Spectrosc. Radiat. Transfer **36**, No. 6, 521–538 (1986).
28. J.M. Hartmann and M.Y. Perrin, Appl. Opt. **28**, 2550–2553 (1989).
29. J.M. Hartmann and C. Boulet, J. Chem. Phys. **94**, No. 10, 6406–6419 (1991).
30. S.D. Tvorogov, Atmos. Oceanic Opt. **8**, Nos. 1–2, 7–13 (1995).
31. D.E. Burch, in: *Semi-Annual Technical Report. Air Force Cambridge Research Lab.*, Publ. U–4784 under contract No. F 19628–69–C–0263 (31 January 1970).